Bimetallic Bi-In Interfaces on Micropyramidal Silicon for Efficient Solar-Driven CO_2-to-Formate Conversion

Manel Machreki, *[a] Marielle Blot, [a] Antoine Vacher, [a] Stéphanie Lamy, [a] and Bruno Fabre*[a]

[a] Univ Rennes, CNRS, ISCR (Institut des Sciences Chimiques de Rennes)-UMR6226, F-35000 Rennes, France.

*Corresponding authors: E-mail: bruno.fabre@univ-rennes.fr; manel.machreki@univ-rennes.fr

1. Experimental Details

1.1. Chemicals and reagents

Formic acid (HCOOH, 99%), Indium (III) nitrate hydrate ($In(NO_3)_3$, H_2O, 99%), Bismuth (III) nitrate pentahydrate (99%, $Bi(NO_3)_3$, 5 H_2O**)**, sulfuric acid (H_2SO_4, 99.7%), nitric acid (HNO_3) and potassium hydrogen bicarbonate ($KHCO_3$, 99%) were purchased from Sigma-Aldrich. All other chemical reagents were of analytical grade and used as received without further purification. For the cleaning and etching of silicon wafers, sulfuric acid (H_2SO_4, 96%, Very Large-Scale Integration (VLSI) grade, Selectipur, VWR) and hydrogen peroxide (H_2O_2, 30%, VLSI grade, Sigma-Aldrich) were used. Additional solvents included acetone (electronic grade MOS, Erbatron, Carlo Erba Reagents) and anhydrous ethanol (RSE electronic grade, Erbatron, Carlo Erba Reagents). All electrolyte solutions were prepared using ultrapure water with a resistivity of 18.2 MΩ·cm (Purelab Flex 2 system, Veolia Water STI).

1.2. Preparation of planar p-Si/SiO_x surfaces

All Teflon vials and tweezers used for silicon cleaning were pre-decontaminated in a 3:1 (v/v) mixture of concentrated H_2SO_4 and 30% H_2O_2 at 105 °C for 30 min, followed by thorough rinsing with ultrapure water.

Caution: Concentrated aqueous H_2SO_4/ H_2O_2 (piranha solution) is highly hazardous, particularly upon contact with organic materials, and must be handled with extreme care.

The *p*-type silicon wafers (5–10 Ω·cm resistivity, 300 ± 25 µm thickness, orientation (100)) were purchased from Electronics. All Si substrates were degreased by sequential sonication in acetone, ethanol, and ultrapure water for 10 min each. The surfaces were subsequently

decontaminated and oxidized in piranha solution at 105 °C for 30 min, rinsed extensively with ultrapure water, and dried under an argon flow.

1.3. Preparation of micropyramidal p-Si surfaces

Micropyramidal silicon arrays were fabricated as follows. After the cleaning procedure described above, the Si surface was etched in HF for 2 min to remove the native oxide layer, followed by rapid drying under an argon stream. An alkaline etching (AE) solution (50 mL) was freshly prepared by dissolving KOH (0.42 M) in a water/isopropanol mixture (5 vol% isopropanol). The planar hydrogenated Si substrate was rinsed thoroughly with ethanol, dried under argon, and immediately immersed in the AE solution for 50 min at 100°C. After etching, the sample was transferred into a beaker containing ultrapure water under stirring to quench the reaction, and subsequently dried under a flow of argon.

1.4. Preparation of micropyramidal p-Si decorated with co-electrodeposited Bi and In catalysts (p-Si/Bi + x mM In)

Electrodeposition of Bi and In catalysts was carried out on freshly hydrogen-terminated micropyramidal *p*-type silicon photocathodes from an aqueous 1 M HNO_3 solution (40 mL) containing 20 mM $Bi(NO_3)_3$, 5 H_2O without and with 0.5, 1 or 10 mM $In(NO_3)_3$, H_2O, via the electroreduction of Bi^{3+} to Bi^0 and In^{3+} to In^0. Prior to deposition, the electrolyte was sonicated and purged with argon for at least 15 min and subsequently maintained under an inert atmosphere. Electrodeposition was performed in a three-electrode configuration with the micropyramidal Si photocathode as the working electrode, a graphite wire as the counter electrode, and a KCl-saturated calomel electrode (SCE) as the reference electrode. The working electrode was immersed in the deposition solution and illuminated using a solar simulator. Photoelectrodeposition was conducted at −0.3 V vs SCE for 30 s. After deposition, the photocathodes were thoroughly rinsed with ultrapure water and dried under a stream of argon. The so prepared photocathodes were abbreviated as *p*-Si/Bi + *x* mM In with *x* = 0, 0.5, 1 and 10.

1.5. Instrumentation

XRD experiments were performed in reflection mode on a Bruker D8 Advance diffractometer equipped with a LynxEye fast detector and working with monochromatized Cu Kα1 radiation (λ = 1.5406 Å).

Reflectance spectra were acquired on a Cary 100 (Varian) spectrophotometer, equipped with an integrating sphere (DRA-CA- 301, Labsphere) referenced with a Spectralon standard (Labsphere). The total reflectance was measured with the surface tilted to include the specular reflectance component.

Scanning electron microscopy (SEM) was performed using a JSM 7100F (JEOL) microscope.

X-ray photoelectron spectroscopy (XPS) data were collected using a NEXSA G2 (Thermo Fisher Scientific) spectrometer equipped with an Al Kα X-ray source operating at 1486.6 eV and a spot size of 200 μm^2. Survey spectra were acquired with a pass energy of 200 eV and a step size of 1 eV, while high-resolution spectra were recorded using a pass energy of 50 eV and a step size of 0.1 eV. All binding energies were referenced to the C 1s peak at 284.8 eV. Core-level spectra of Bi 4f, In 3s, and O 1s were peak-fitted using CasaXPS software (version 2.3.18), employing either a Tougaard or Shirley background for spectral analysis.

High-performance liquid chromatography (HPLC) measurements were performed using an Agilent 1200 HPLC system equipped with a variable wavelength detector (VWD, UV). A 100 μL aliquot of the post-electrolysis electrolyte was diluted to 1 mL with diluted H_2SO_4 solution and filtered prior to analysis. Subsequently, 20 μL of the prepared sample was injected into a Bio-Rad Aminex HPX-87H column. A 5 mM H_2SO_4 solution was used as the mobile phase at a constant flow rate of 0.6 mL min^{-1}. The concentration of formate was determined from calibration curves obtained using standard solutions of known concentrations.

Gas-phase products were analysed by gas chromatography (GC) using an Agilent 7890B gas chromatograph equipped with a thermal conductivity detector (TCD) for permanent gases (e.g., H_2, CO). Gas samples were periodically withdrawn from the headspace of the electrochemical cell using a gas-tight syringe and injected into the GC. Separation was carried out using a molecular sieve 5Å column with high-purity argon (Ar) as the carrier gas. The concentrations of gaseous products were determined by comparing the peak areas with calibration curves obtained from standard gas mixtures of known composition.

1.6. Photoelectrochemical measurements

For photoelectrochemical measurements, the bare *p*-Si and *p*-Si/Bi + *x* mM In (with $x = 0$, 0.5, 1 and 10) surfaces were further processed to fabricate photocathodes. An ohmic contact was established on the backside of the Si surface with a metal wire by first scrubbing the surface with a diamond glass cutter and then applying a droplet of InGa eutectic (99.99%, Alfa Aesar).

A layer of silver paste (Electron Microscopy Sciences) was then deposited on the contact. After drying of the silver paste, the metal wire was inserted in a glass capillary, and the electrode area (~0.2-0.5 cm^2) was defined with an epoxy-based resin (Loctite 9460, Henkel) that covered all the backside of the Si surface as well as the silver paste.

The (photo)electrochemical measurements were performed at room temperature using a three-electrode configuration on a BioLogic SP-200 electrochemical workstation (single-channel). An aqueous 0.5 M $KHCO_3$ solution was used as the electrolyte; the pH was 8.3 under Ar saturation and ~7.2 under CO_2 saturation. Illumination was provided by a solar simulator (LS0106, LOT Quantum Design) with a fluence of 100 mW cm^{-2}, equipped with an AM 1.5G filter. A three-electrode setup was employed for the PEC experiments, where the *p*-Si/Bi + *x* mM In photocathode served as the working electrode (geometric area ~0.15–0.20 cm^2), a saturated calomel electrode (SCE) was used as the reference electrode and a DSA (dimensionally stable anode: RuO_2 on Ti substrate, from ECS Tarn) electrode acted as the counter electrode. To express a reference electrode potential versus the reversible hydrogen electrode (RHE), the standard conversion is:

$$E_{RHE} = E_{SCE} + 0.059\ pH + E^0_{SCE} \text{ with } E^0_{SCE} = 0.241\ V \quad (1)$$

where E_{SCE} is the applied potential versus the used reference electrode.

2. Mott-Schottky (M-S) Analysis

The Mott–Schottky analysis was performed over 1–10 kHz, and the high-frequency region was used for comparison to minimize the contribution of slow surface/interface states. The flat-band potential V_{FB} can be obtained from the M–S plot based on Eq. (2):[1]

$$\frac{1}{C^2} = \frac{2}{\varepsilon\varepsilon_0 e N_A A^2}\left(V_{FB} - V - \frac{kT}{e}\right) \quad (2)$$

where ε is the dielectric constant of Si ($\varepsilon = 11.7$), ε_0 is the vacuum permittivity, e is the elementary charge, N_A is the acceptor density, A is the electrode area, V is the applied potential, k is the Boltzmann constant, and T is the absolute temperature. The same geometric electrode area was used for capacitance normalization for all electrodes. The possible frequency dispersion at low frequency may arise from surface/interface states and additional interfacial

capacitance associated with the catalyst layer. Accordingly, V_{FB} was estimated from the intercept of the linear region of the M-S plots, while the apparent acceptor density was obtained from the slope according to Eq. (3):

$$N_A = \frac{2}{\varepsilon\varepsilon_0 e A^2}\left(\frac{d(1/C^2)}{dV}\right)^{-1} \quad (3)$$

3. Calculations of the Faradaic Efficiency

The Faradaic efficiencies (FE) for H_2 and $HCOO^-$ were calculated using the following equation (4):

$$FE = \left(\frac{n \times z \times F}{Q}\right) \times 100 \quad (4)$$

where n is the amount of produced H_2 or $HCOO^-$ (in mole), z is number of mole of electrons transferred per mole of product, Q is the consumed total charge (in C), and F is the Faraday constant (96485 C mol^{-1}).

The hydrogen evolution reaction (HER) can be written as:

$$2H_2O + 2e^- \rightarrow H_2 + 2OH^- \quad (5)$$

Therefore, $z = 2$ for H_2 production.

The electrochemical reduction of CO_2 to formate can be written as:

$$CO_2 + H_2O + 2e^- \rightarrow HCOO^- + OH^- \quad (6)$$

Therefore, $z = 2$ for $HCOO^-$ production. Thus, two electrons are involved per mole of both H_2 and $HCOO^-$ formed.

4. Additional Figures and Tables

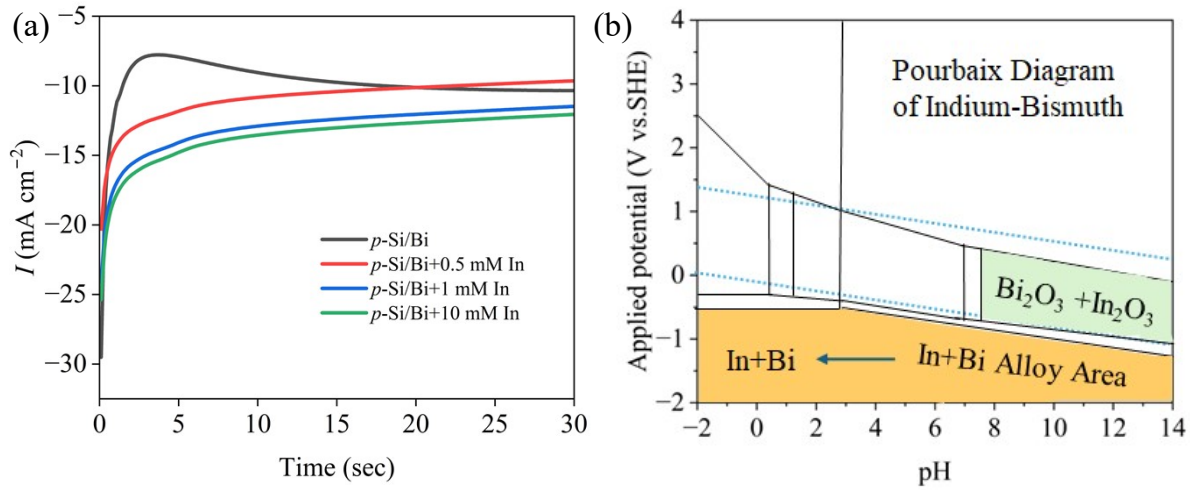

Fig. S1. (a) Chronoamperometry curves recorded during Bi^0 and Bi^0 + In^0 electrodeposition at −0.3 V *vs* Saturated Calomel Electrode (SCE) on illuminated freshly hydrogenated *p*-type Si photocathodes. Electrodeposition solution: aqueous 1 M HNO_3 solution containing 20 mM Bi $(NO_3)_3$, 5 H_2O without and with 0.5, 1 or 10 mM $In(NO_3)_3$, H_2O. *I* is the cathodic photocurrent density. (b) Pourbaix diagram of indium−bismuth system.[2]

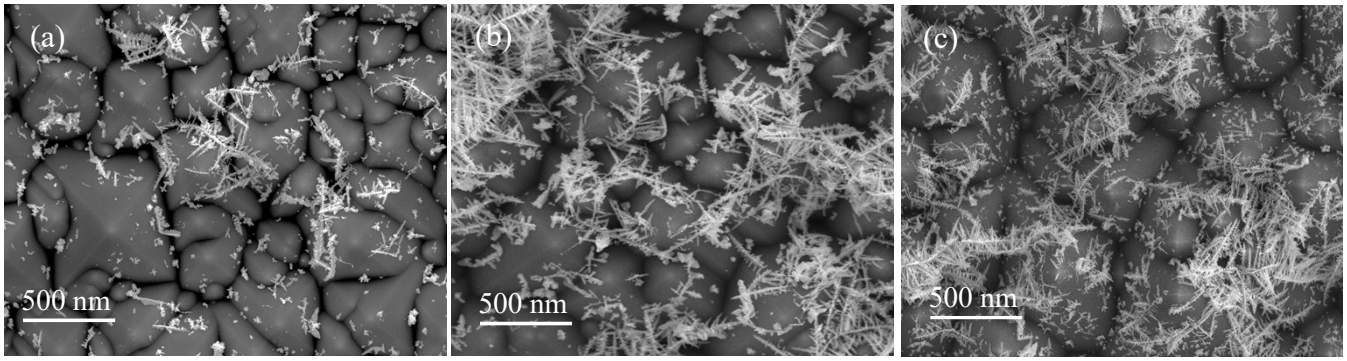

Fig. S2. Top-view SEM images of (a) *p*-Si/Bi, (b) *p*-Si/Bi + 1 mM In, and (c) *p*-Si/Bi + 10 mM In.

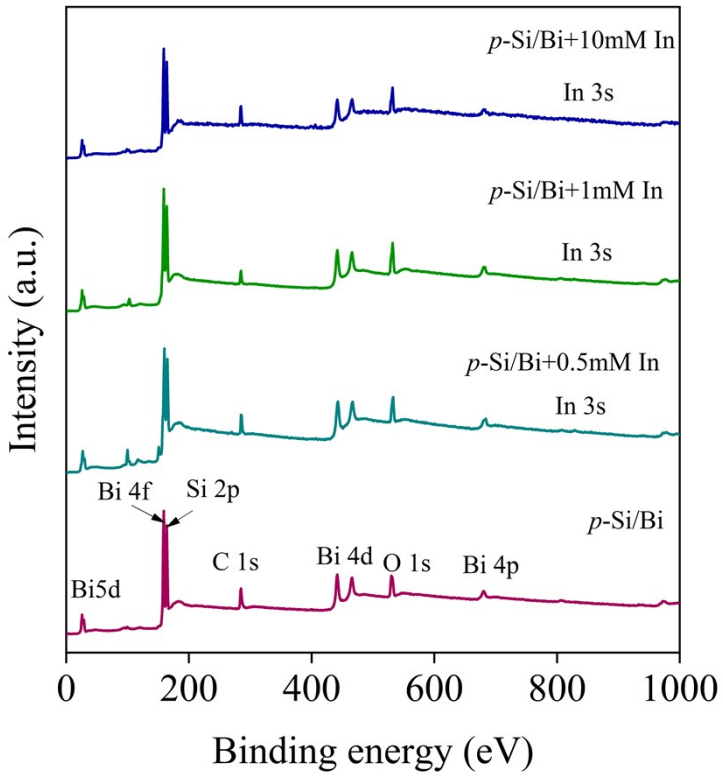

Fig. S3. Survey XPS spectra of *p*-Si/Bi + *x* mM In (*x* = 0, 0.5, 1 and 10) surfaces.

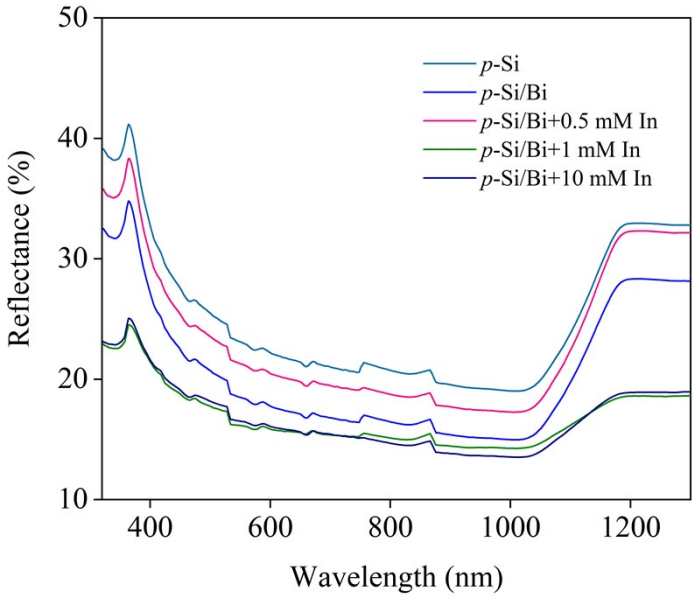

Fig. S4. Total reflectance spectra of *p*-Si and *p*-Si/Bi + *x* mM In (*x* = 0, 0.5, 1 and 10) surfaces.

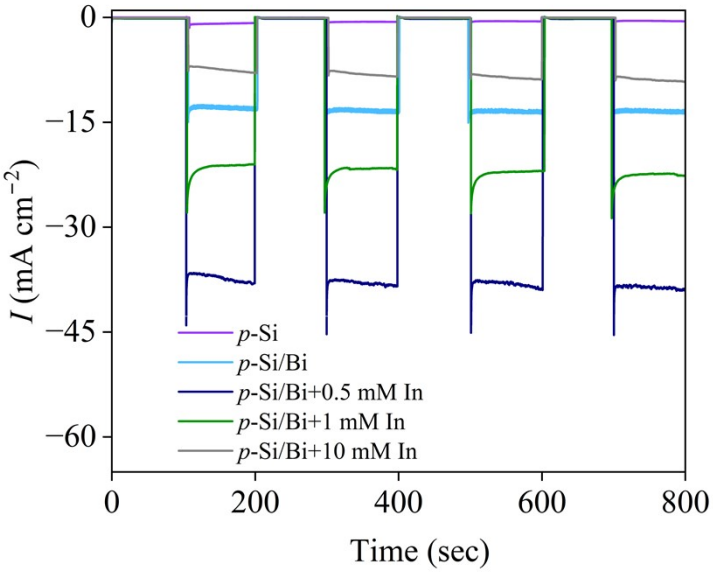

Fig. S5. Current–time (*I*–*t*) curves of *p*-Si and *p*-Si/Bi + *x* mM In (*x* = 0, 0.5, 1 and 10) photocathodes recorded at –0.8 V vs RHE under chopped illumination in CO_2-saturated 0.5 M $KHCO_3$ solution.

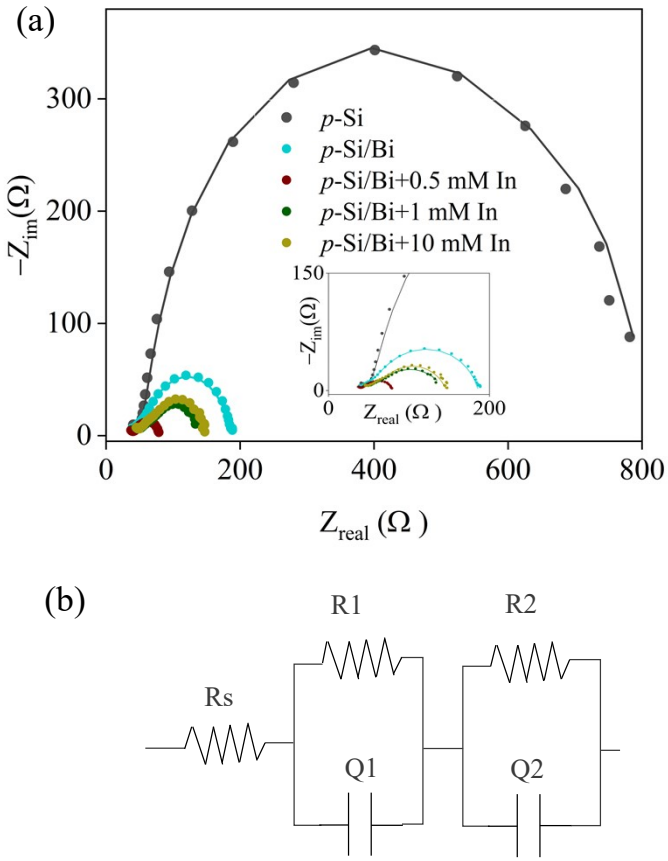

Fig. S6. (a) Nyquist plots of *p*-Si and *p*-Si/Bi + *x* mM In (*x* = 0, 0.5, 1 and 10) photocathodes recorded at –0.7 V vs RHE under illumination in Ar-saturated 0.5 M $KHCO_3$ solution. The

inset shows a zoomed view of the low-impedance region. (b) Equivalent electrical circuit model used to fit the EIS spectra.

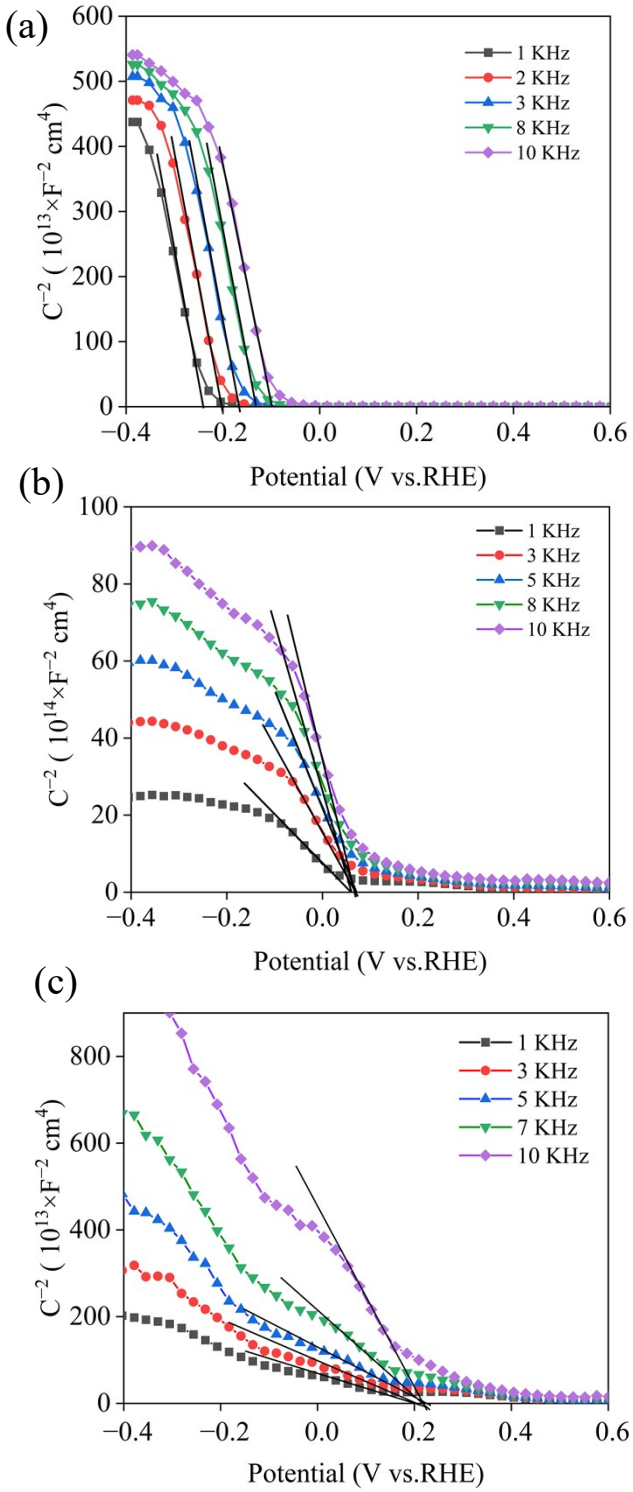

Fig. S7. Mott–Schottky (M–S) C^{-2} - E plots measured at different frequencies in Ar-saturated 0.5 M $KHCO_3$ of (a) *p*-Si, (b) *p*-Si/Bi and (c) *p*-Si/Bi + 0.5 mM In surfaces in the dark. *All samples exhibit negative slopes, consistent with the p-type character of the silicon substrate.*

The apparent N_A values derived from the M–S slopes are in the range 1.4-1.8 × 10^{15} cm^{-3} and are relatively in good agreement with the resistivity value given by the wafer manufacturer (5-10 Ω cm). (Table S4).

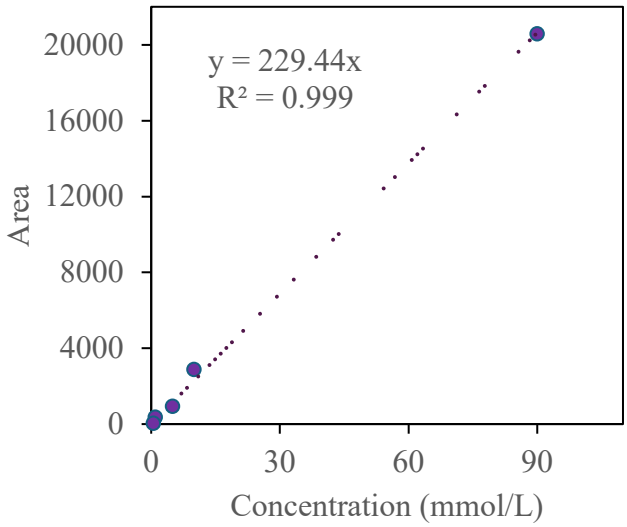

Fig. S8. Calibration curve between integrated chromatogram peak area and the formic acid (FA) concentration.

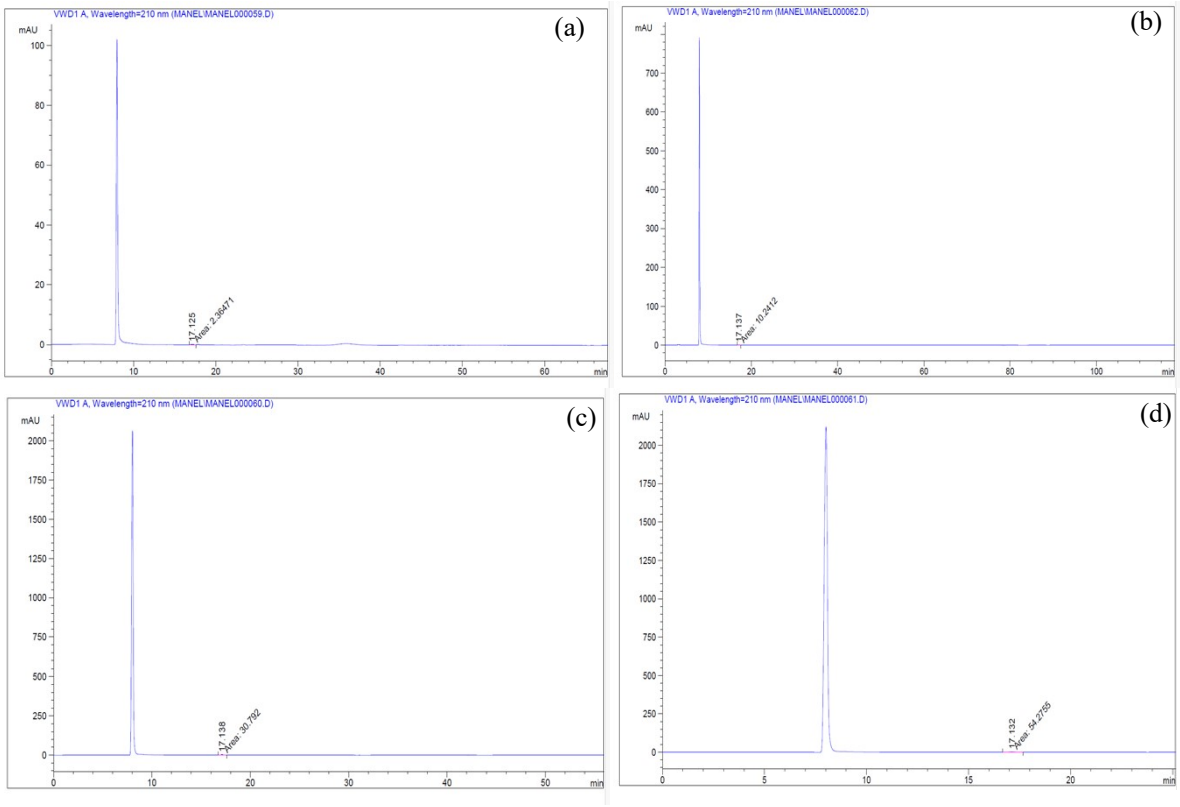

Fig. S9. HPLC chromatograms recorded after 60 min electrolysis of *p*-Si/Bi + 0.5 mM In photocathodes at (a) −0.1, (b) −0.3, (c) −1.0 and (d) −1.5 V vs RHE in Ar-saturated 0.5 M $KHCO_3$ solution under illumination. The intense peak at ~17.1 min corresponds to FA.

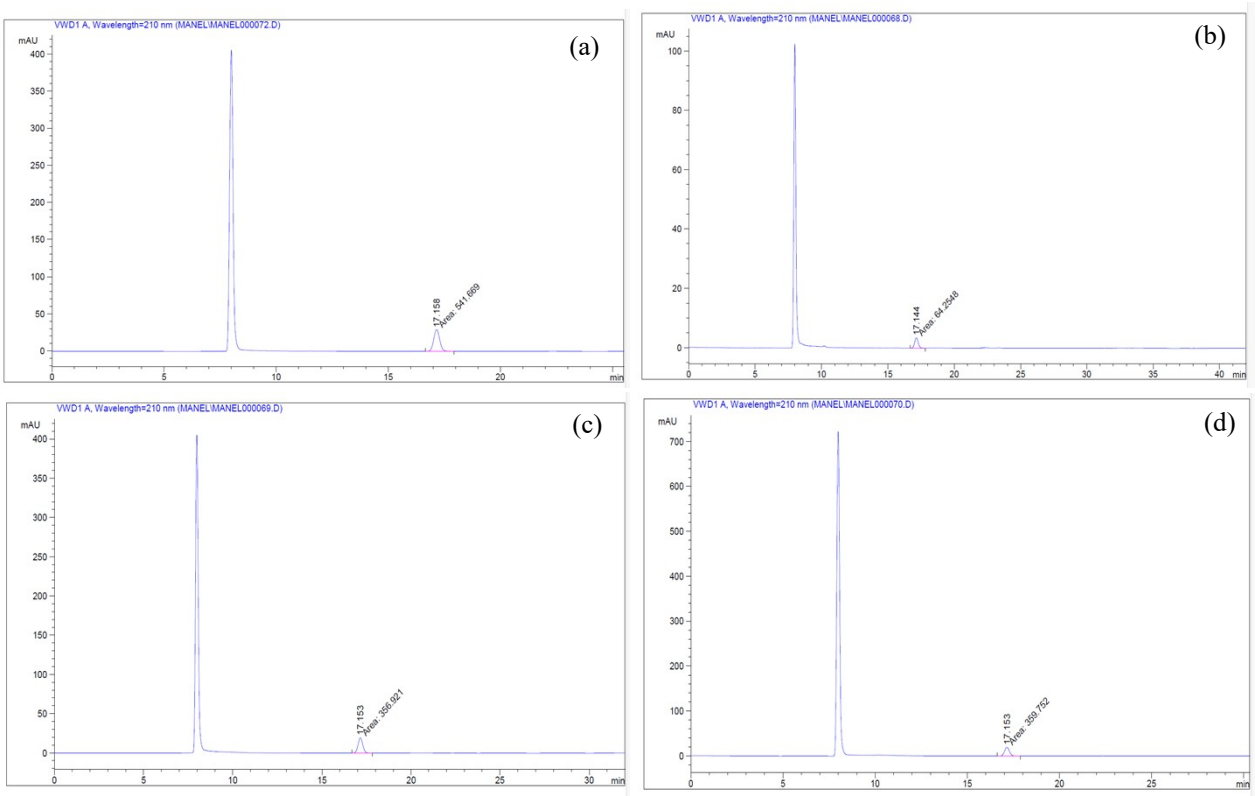

Fig. S10. HPLC chromatograms recorded after 60 min electrolysis of *p*-Si/Bi + 0.5 mM In photocathodes at (a) –0.1, (b) –0.3, (c) –1.0 and (d) –1.5 V vs RHE in CO_2-saturated 0.5 M $KHCO_3$ solution under illumination. The intense peak at ~17.1 min corresponds to FA.

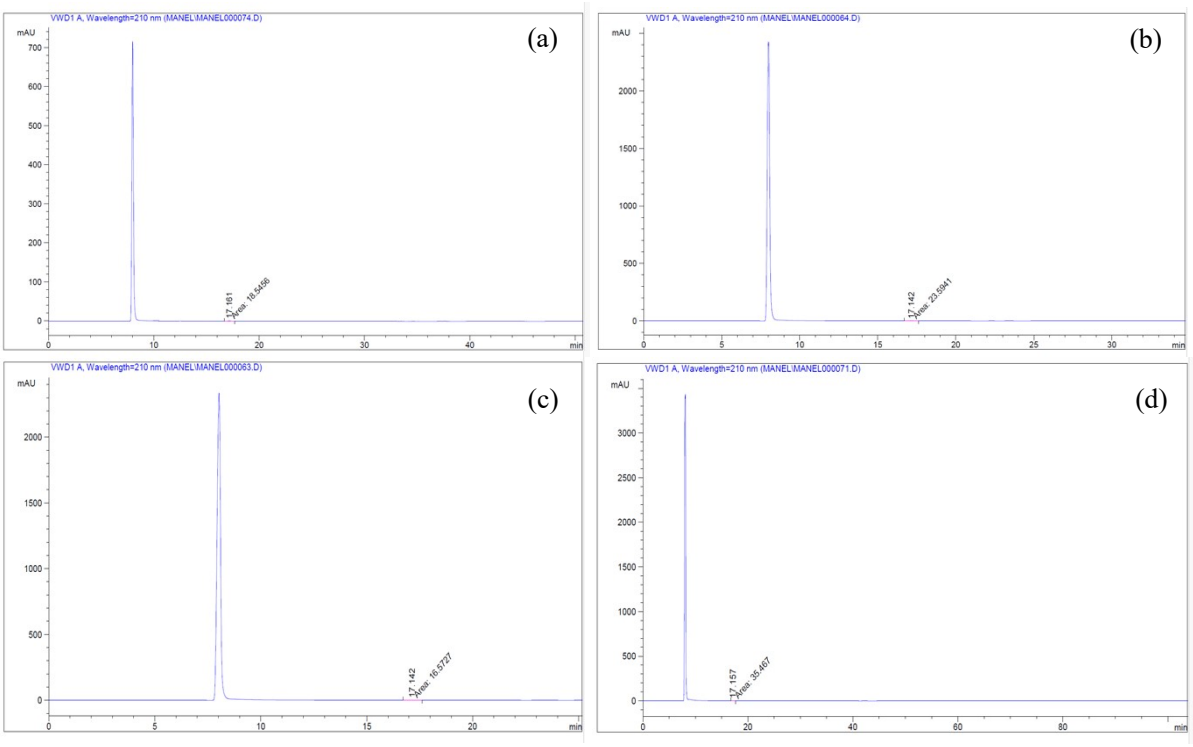

Fig. S11. HPLC chromatograms recorded after 60 min electrolysis of (a) *p*-Si/Bi, (b) *p*-Si/Bi + 0.5 mM In, (c) *p*-Si/Bi + 1 mM In and (d) *p*-Si/Bi + 10 mM In photocathodes at –0.7 V vs RHE in Ar-saturated 0.5 M $KHCO_3$ solution under illumination. The intense peak at ~17.1 min corresponds to FA.

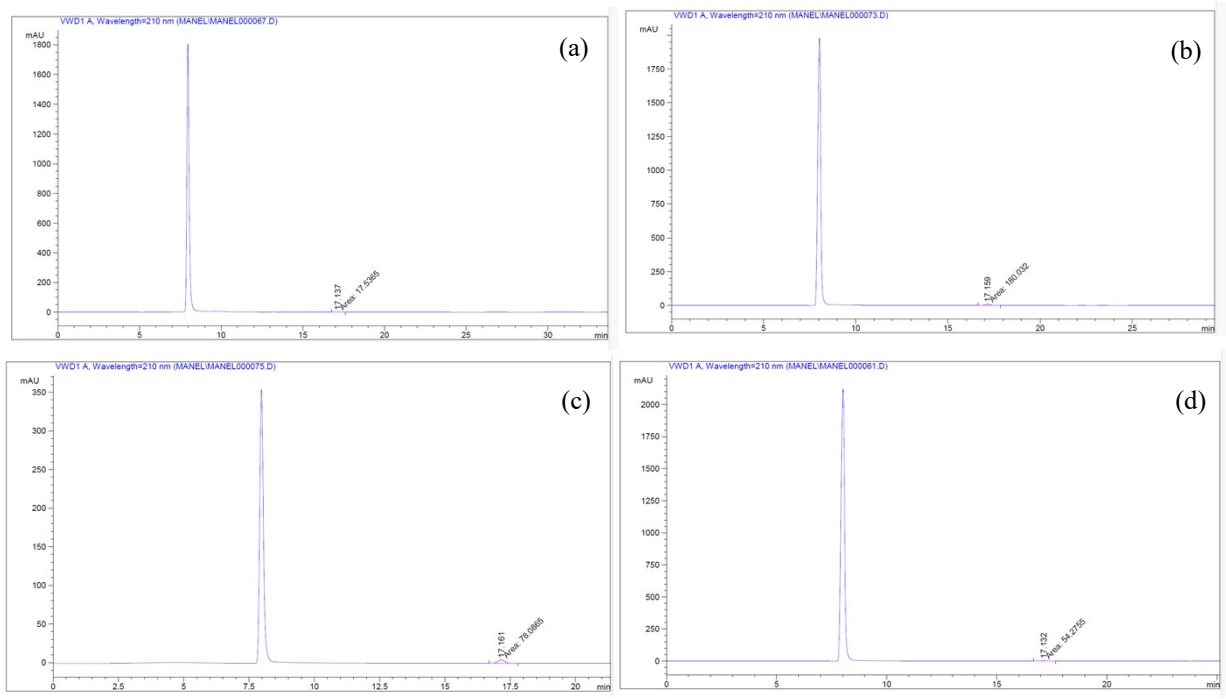

Fig. S12. HPLC chromatograms recorded after 60 min electrolysis of (a) *p*-Si/Bi, (b) *p*-Si/Bi + 0.5 mM In, (c) *p*-Si/Bi + 1 mM In and (d) *p*-Si/Bi + 10 mM In photocathodes at –0.7 V vs RHE in CO_2-saturated 0.5 M $KHCO_3$ solution under illumination. The intense peak at ~17.1 min corresponds to FA.

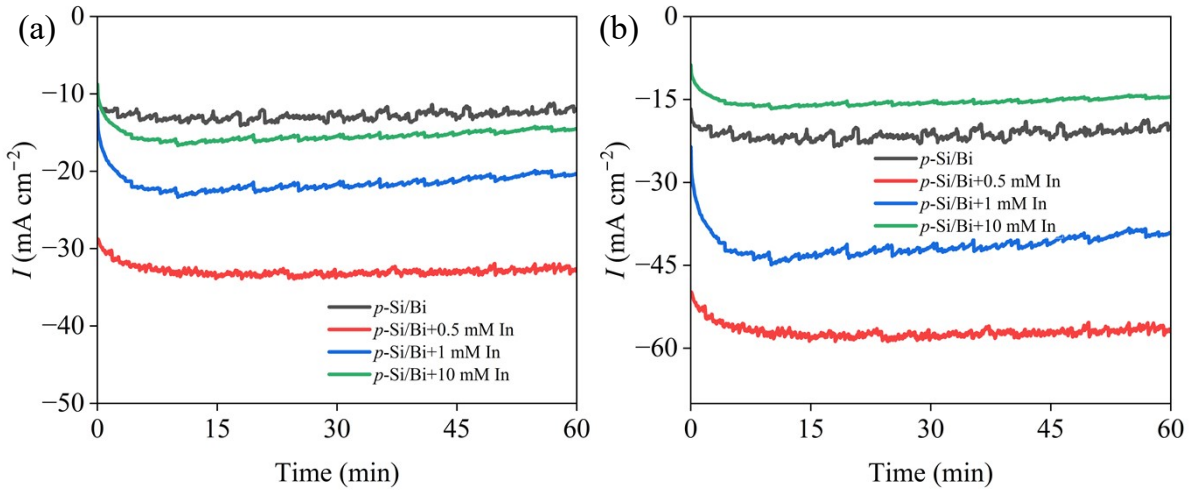

Fig. S13. Chronoamperometry ($I - t$) curves of *p*-Si/Bi + *x* mM In (*x* = 0, 0.5, 1 and 10) photocathodes recorded at –0.7 V vs RHE in (a) Ar- and (b) CO_2-saturated 0.5 M $KHCO_3$ solution under illumination.

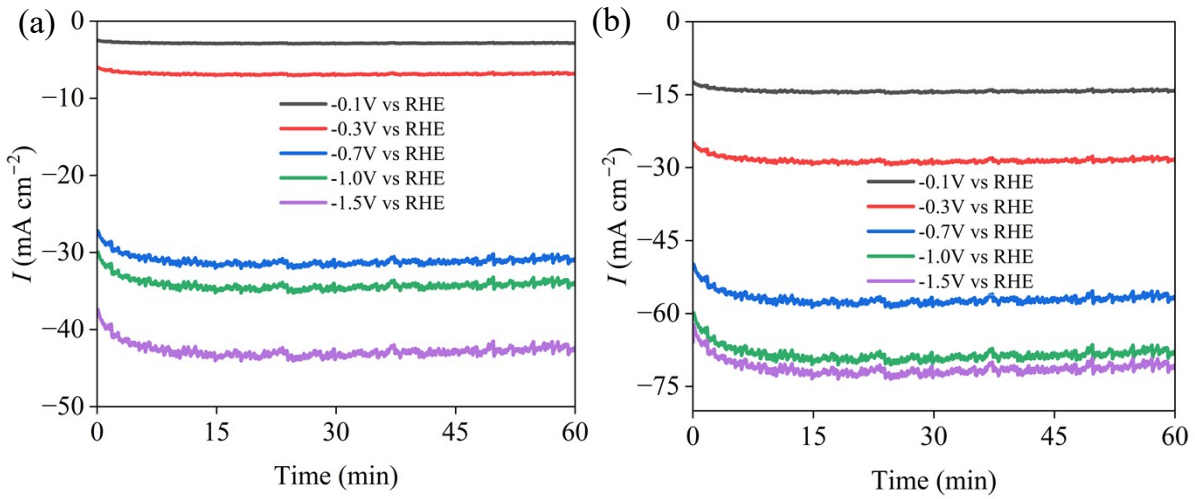

Fig. S14. Chronoamperometry ($I - t$) curves of p-Si/Bi + 0.5 mM In photocathodes recorded at different potentials in (a) Ar- and (b) CO_2-saturated 0.5 M $KHCO_3$ solution under illumination.

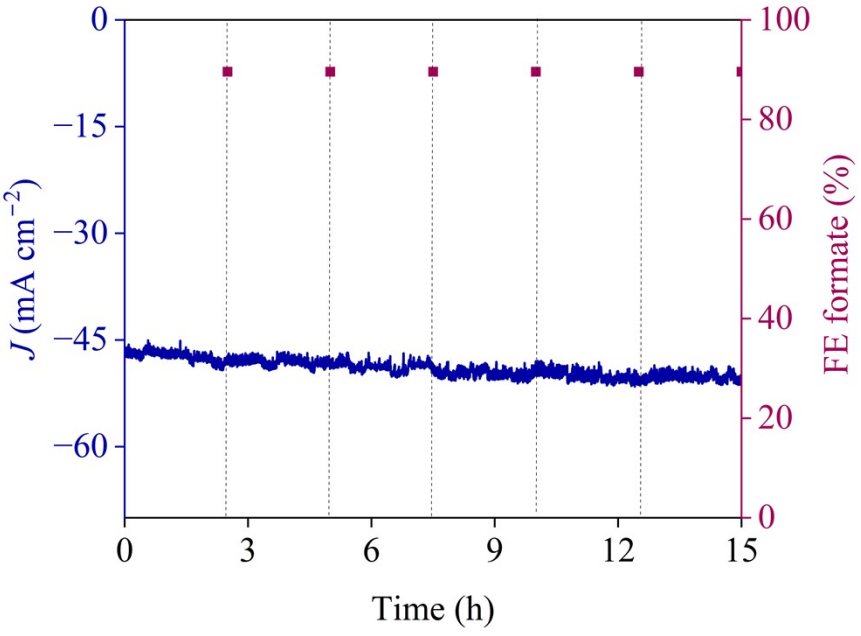

Fig. S15. Chronoamperometry ($j - t$) curve and evolution of FE for formate of p-Si/Bi + 0.5 mM In photocathode recorded at –0.7 V vs RHE for 15 hours in CO_2-saturated 0.5 M $KHCO_3$ solution under illumination.

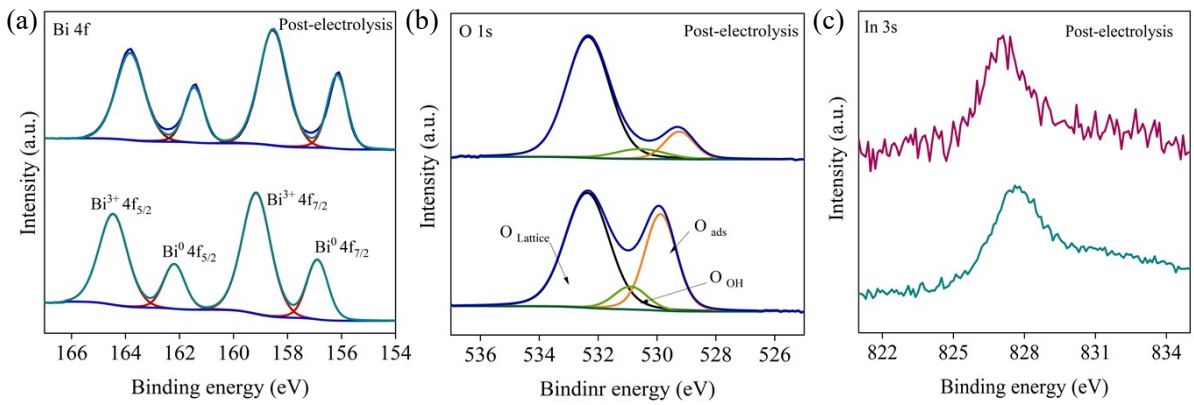

Fig. S16. XPS spectra for (a) Bi 4f, (b) O 1s and (c) In 3s regions of *p*-Si/Bi + 0.5 mM In photocathode recorded before and after the PEC long stability test (15 h) at –0.7 V vs RHE in CO_2-saturated electrolyte under illumination.

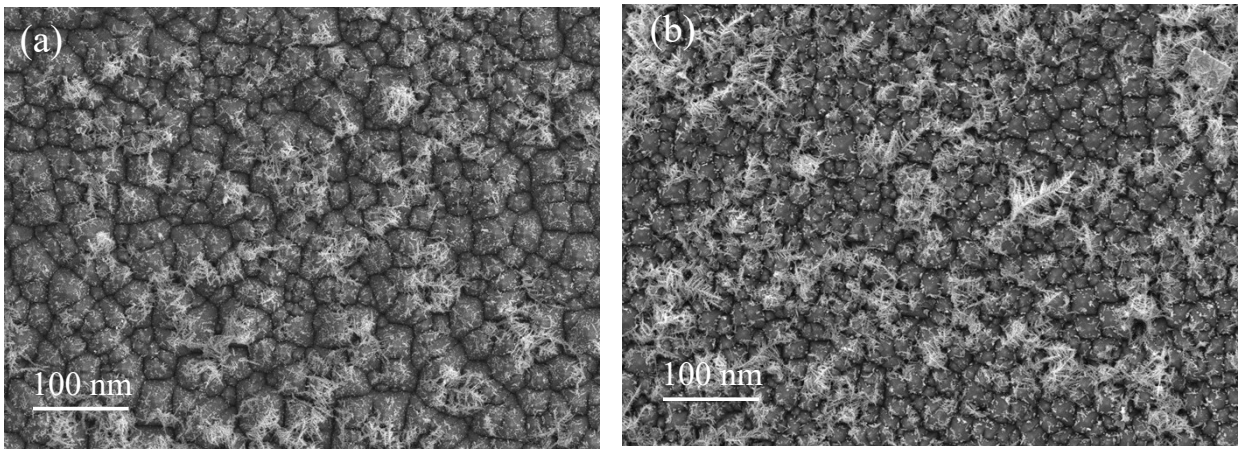

Fig. S17. SEM images of the *p*-Si/Bi + 0.5 mM In photocathode recorded (a) before and (b) after the 15 h PEC stability test at −0.7 V vs RHE in CO_2-saturated 0.5 M $KHCO_3$ electrolyte under illumination.

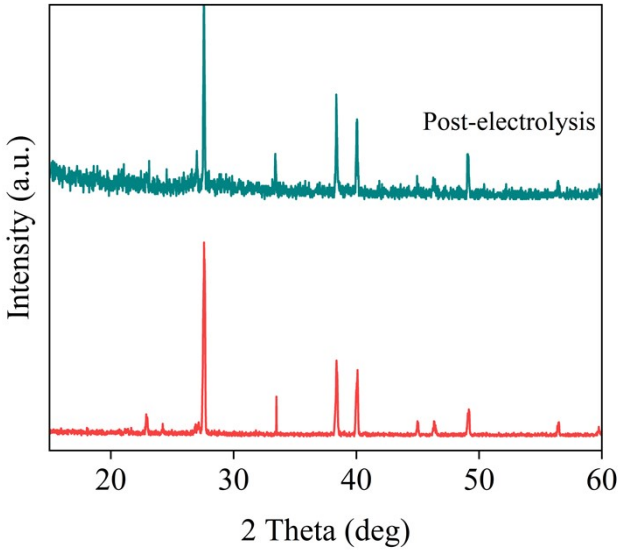

Fig. S18. XRD patterns of *p*-Si/Bi + 0.5 mM In photocathode recorded before and after the PEC long stability test (15 h) at –0.7 V vs RHE in CO_2-saturated electrolyte under illumination.

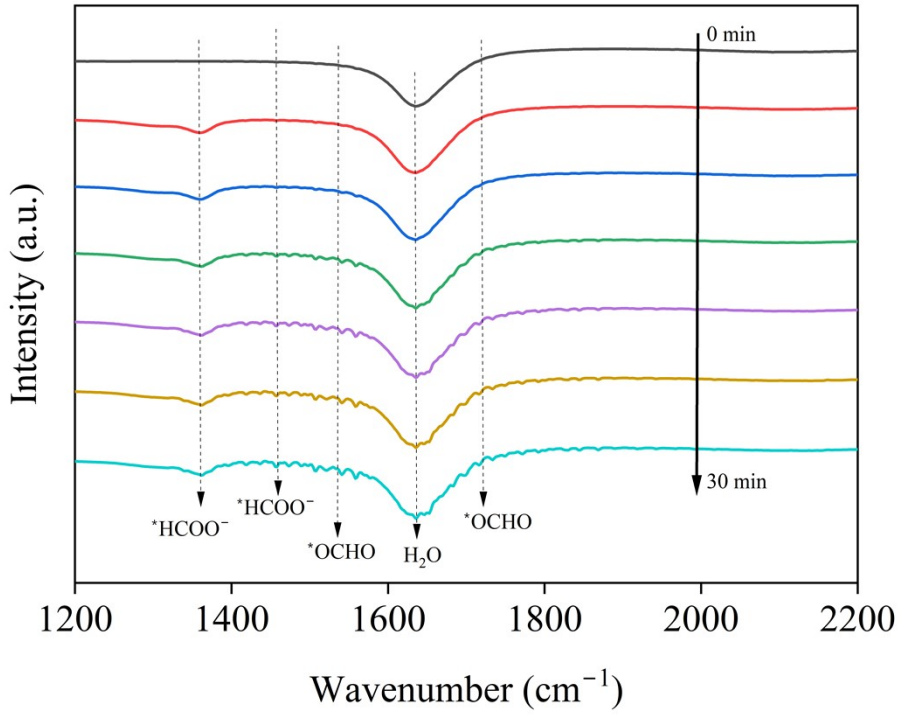

Fig. S19. *In situ* ATR-FTIR spectra recorded as a function of reaction time during PEC CO_2 reduction on the *p*-Si/Bi + 0.5 mM In photocathode from 0 to 30 min under illumination at −0.7 V vs RHE.

Table S1. Atomic percentages of Bi, In, O and Si elements from XPS spectra for the catalytic films.

Samples	Bi (%)	In (%)	O (%)	Si (%)
***p*-Si/Bi**	10.5	–	33.4	12.7
***p*-Si/Bi + 0.5 mM In**	10.0	0.13	29.7	20.8
***p*-Si/Bi + 1 mM In**	11.0	0.4	29.0	21.5
***p*-Si/Bi + 10 mM In**	11.2	0.94	30.1	11.6

Table S2. Onset potential (V vs RHE) measured at –0.5 mA cm^{-2}.

Photocathode	Ar gas	CO_2 gas
***p*-Si/Bi**	–0.44	–0.30
***p*-Si/Bi + 0.5 mM In**	–0.25	+0.06
***p*-Si/Bi + 1 mM In**	–0.33	–0.20
***p*-Si/Bi + 10 mM In**	–0.60	–0.50

Table S3. Series resistance of the electrolyte and the substrate layer (R_s), the bulk charge transfer resistance ($R_{ct\text{-}bulk}$) and the trap-related charge transfer resistance ($R_{ct\text{-}trap}$) of the photocathodes, determined from EIS measurements.

Photocathode	R_s (Ω)	$R_{ct,bulk}$ (Ω)	$R_{ct,trap}$ (Ω)
***p*-Si**	9.31	44.06	784.87
***p*-Si/Bi**	22.47	67.72	61.96
***p*-Si/Bi + 0.5 mM In**	2.76	37.38	40.98
***p*-Si/Bi + 1 mM In**	35.46	42.01	70.02
***p*-Si/Bi + 10 mM In**	29.79	113.02	44.41

Table S4. Parameters extracted from Mott-Schottky analysis of *p*-Si, *p*-Si/Bi, and *p*-Si/Bi + 0.5 mM In in Ar-saturated 0.5 M $KHCO_3$ solution in the dark.

Electrode	Frequency (kHz)	V_{FB} (V vs RHE)	N_A (cm^{-3})
***p*-Si**	1	-0.26	1.57×10^{15}
	3	-0.22	1.40×10^{15}
	5	-0.19	1.45×10^{15}
	8	-0.16	1.35×10^{15}
	10	-0.10	1.44×10^{15}
***p*-Si/Bi**	1	0.04	1.8×10^{15}
	3	0.04	1.7×10^{15}
	5	0.04	1.5×10^{15}
	8	0.04	1.6×10^{15}
	10	0.04	1.8×10^{15}
***p*-Si/Bi + 0.5 mM In**	1	0.17	1.23×10^{15}
	3	0.17	1.53×10^{15}
	5	0.19	1.72×10^{15}
	8	0.19	1.84×10^{15}
	10	0.19	1.64×10^{15}

Table S5. FE for H_2 (%) measured for different photocathodes electrolysed for 60 min at -0.7 V vs. RHE in 0.5 M $KHCO_3$ solution under illumination.

Photocathode	Ar gas	CO_2 gas
***p*-Si/Bi**	94.7	81.4
***p*-Si/Bi + 0.5mM In**	93.4	10.4
***p*-Si/Bi + 1 mM In**	93.9	51.5
***p*-Si/Bi + 10 mM In**	95.5	79.6

Table S6. FE for H_2 (%) measured for *p*-Si/Bi + 0.5 mM In photocathode electrolysed for 60 min at different applied potentials in 0.5 M $KHCO_3$ solution under illumination.

Applied potential (V vs RHE)	Ar gas	CO_2 gas
-0.1	99.5	68.6
-0.3	97.7	40.7
-0.7	93.4	10.4
-1.0	90.1	8.8
-1.5	83.2	4.8

Table S7. Comparison among state-of-the-art Bi-decorated Si-based photoelectrodes for the formate production from PEC CO_2 reduction.

Semiconductor/catalyst	Catalyst synthesis and deposition	Electrolyte	Applied potential	FE for formate (%)	Ref
p-Si/Bi + 0.5 mM In	Photoelectrodeposition on pyramidal *p*-Si	0.5 M $KHCO_3$	−0.7 V vs. RHE	89.6	**This work**
p-Si nanowires/Bi–Sn	Co-catalyst modification on *p*-Si nanowires arrays	0.1 M $KHCO_3$	−1.02 V vs. RHE	88.7	3
p-Si/ZnO/Bi–Bi_2O_3	Hydrothermal growth + electrodeposition	0.1 M $KHCO_3$	−0.95 V vs. RHE	84.3	4
p-Si/Bi_2O_3	Bi photoelectrodeposition on *p*-Si photocathode	0.5 M $KHCO_3$	−1.4 V vs. RHE	73	5
p-Si/GaN/Bi	Bi nanoparticles supported on GaN/Si photocathode	0.5 M $KHCO_3$	−0.2 V vs. RHE	85.2	6

p-Si nanowires/porous carbon nanorods/Bi	Hydrothermally prepared C nanorods embedding Bi nanoparticles + drop coating of the catalytic ink with Nafion	0.1 M $KHCO_3$	−0.9 V vs. RHE	91.2	7
p-Si microwires/ultra-long Bi nanowires	Hydrothermally prepared Bi_2O_3 nanowires + electrochemical reduction on deep reactive ion etching (DRIE)-prepared tapered Si microwires	0.1 M $KHCO_3$	−0.5 V vs. RHE	87	8

4. References

1. X. G. Zhang, *Electrochemistry of Silicon and its Oxide*; Kluwer Academic Publishers: New York, 2004.
2. Y. Hu, Y. Li, B. Yao, G. Sun, F. Yu, C. Chi, C. Zhang, T. Liu, P. Zhang, H. Li, Q. He, J. Zhang and A. B. Wong, *ACS Catal*., 2025, **15**, 13260-13277.
3. W. Shen, Z. Yang, J. Wang, J. Cui, Z. Bao, D. Yu, M. Guo, G. Xu and J. Lv, *ACS Sustainable Chem. Eng.*, 2023, **11**, 13451–13457.
4. Q. Zhang, X. Zhou, Z. Kuang, Y. Xue, C. Li, M. Zhu, C.-Y. Mou and H. Chen, *ACS Sustainable Chem. Eng.*, 2022, **10**, 2380–2387.
5. D. Fu, J. Tourneur, B. Fabre, G. Loget, Y. Lou, F. Geneste, S. Ababou-Girard and C. Mériadec, *ChemCatChem*, 2020, **12**, 5819–5825.
6. Y. Pan, X. Zhang, C. Liu, J. Shi, Y. Chen, H. Li, M. Guo, J. Yang and S. Chu, *Nat. Commun.*, 2023, **14**, 1013.
7. Y. Chen, J. Kang, M. Zou, K. Wang, M. Liu and W. Li, *Ind. Eng. Chem. Res*., 2024, **63**, 21831−21840.
8. D. Seo, Y.-I. Kim, J. Son, S. Park, D. Oh, J. Jang, H.-D. Um, H. Shin, K. M. Nam, *Small*, 2026, **22**, e14138.